IIETA International Information and Engineering Technology Association
Advancing the World of Information and Engineering

Annales de Chimie - Science des Matériaux
Vol. 48, No. 3, June, 2024, pp. 417-425
Journal homepage: http://iieta.org/journals/acsm

Characterization and Utilization of Wood Ash in Geopolymers Production and Pb^{+2} Removal from an Aqueous Solution

Faten Al-Slaty[1*], Madlin Amjad[1], Islam Al-Dabsheh[2], Enas N. Mahmoud[3]

[1] Department of Earth and Environmental Sciences, The Hashemite University, Zarqa 13133, Jordan
[2] Department of Applied Geology and Environmental Sciences, Institute of Earth and Environmental Sciences, Al al-Bayt University, Mafraq 25113, Jordan
[3] Department of Chemistry, Faculty of Science, The Hashemite University, Zarqa 13133, Jordan

Corresponding Author Email: fatenm@hu.edu.jo

https://doi.org/10.18280/acsm.480314

Received: 24 January 2024
Revised: 11 May 2024
Accepted: 4 June 2024
Available online: 30 June 2024

Keywords:
alkali activation, geopolymers, wood ash, clay materials, kaolin, Pb^{+2} removal, adsorption

ABSTRACT

The main goal of this work is to characterize wood ash as a waste product from tree trunks burning and utilize it for geopolymer production. The geopolymerization was achieved by a chemical reaction between calcined kaolin and different ratios of wood ash in an alkali solution of sodium silicate (Na_2SiO_3) and sodium hydroxide (NaOH). The produced geopolymers' physical, chemical, and microstructural characteristics were investigated. The synthesized geopolymer with 50% wood ash showed lower density, higher water absorbability, and higher porosity than the free wood ash geopolymer. The microstructural analysis indicated the formation of zeolitic and amorphous phases that were causing an increase in micropores and a high specific surface area, as revealed by XRD, SEM, and BET analyses. Therefore, the potential use of the developed geopolymer for Pb^{+2} removal from an aqueous solution was investigated. It was found that the generated geopolymer has a higher removal efficiency than the raw materials. The studied adsorption isotherms showed that the Langmuir isotherm model explains the experimental results well than the Freundlich model.

1. INTRODUCTION

Wood ash is a light by-product of wood combustion for energy production. Wood ash is an alkaline material with pH ranging from 8 to 13. Wood ash contains micro and macro nutrients extracted from the soil during tree growth [1]. The main properties of the wood ash vary significantly based on the type of trees, the method of combustion, and the boiler's efficiency [2]. Since wood is a significant natural source for different uses in our lives, there is an increase in the amount of wood ash waste generated. Approximately 70% of the generated wood ash is landfilled [3]. Since then, developing practical applications for wood ash has become vital for solving the issues regarding its disposal. Etiegni and Campbell [4] reported that wood ash is widely used as a replacement for lime in solidifying hazardous wastes, for odour control, and for pH control of hazardous and non-hazardous wastes. Numerous studies have demonstrated that wood ash applications as a soil amendment improve tree growth [5-8]. Many researchers showed the possibility of using wood ash in construction materials as supplementary cementitious material [9-13]. Wood ash is also used to prepare light bricks [14-17].

Geopolymer is an inorganic product with a three-dimensional structure produced through the chemical reaction of an alkaline solution with low-cost aluminium silicate components. It has high mechanical properties and is environmentally friendly. Geopolymers are widely used in construction applications. Some materials used in geopolymer production, such as fly ash, volcanic ash, zeolitic tuff, blast furnace slag, and others, provide the geopolymer mortars with a high porosity and large specific surface area, which enhances their adsorption capacity for various pollutants.

Many researchers have recently investigated the suitability of wood ash as a replacement material for the production of sustainable geopolymeric pastes, including Temuujin et al. [18], Cheah et al. [19, 20], Candamano et al. [21], Abdulkareem et al. [22], Owaid et al. [23], and Silvestro et al. [24]. Based on Teker Ercan et al. [25], adding wood ash for geopolymer paste increased the porosity of the binder matrix. Rajamma et al. [26] prepared geopolymer mortars from wood ash and metakaolin. They found that wood ash works well in the alkali activation and is more potent than mortars with only wood ash. Candamano et al. [21] assessed the influence of wood ash as a partial replacement in metakaolin-based geopolymer mortars. They found that the addition of wood ash caused a decrease in compression strength, increased the workability of the mortars, increased porosity, and increased drying shrinkage values. Bijeljić et al. [27] mixed wood and fly ashes to produce geopolymer paste and prepared mortars for concrete with wood ash proportion. They investigated the influence of adding wood ash on geopolymer mortars' mechanical properties and durability. They observed that wood ash and fly ash display beneficial pozzolanic activity. On the other hand, the mixtures prepared with 20% wood ash added showed better sulfate resistance than those prepared only with fly ash. Prabhakar et al. [28] investigated using

wood ash in geopolymer production to absorb iron and lead in wastewater. The adsorption pattern is compatible with the Langmuir isotherm, indicating a high removal efficiency.

This study differs from previous work. It is environmentally significant and has potential industrial value by resolving the issues around wood ash disposal. In addition to developing environmental uses for wood ash in aqueous solutions for heavy metals adsorption, minimal research has been done. The first object of the present work is to characterize wood ash produced by burning different wood tree types in home stoves. The second object is to utilize wood ash in geopolymer production as an additive material in preparation. The third one is studying the utility of the prepared geopolymer in Pb^{+2} removal from an aqueous solution. Lead was selected in this study because of its toxicity; its removal from water and wastewater is essential for human health.

2. MATERIALS AND METHODS

2.1 Raw materials

For the geopolymer synthesis, a kaolin sample (k) was collected from the Ma`an area in south Jordan, approximately 110 km NE of Amman. Wood ash (Wa) was collected from a home fireplace from burning different wood tree types. Wa was sieved to a grain size under 75 µm. The kaolin sample was crushed by a mechanical crusher to a smaller size, sieved to less than 75 µm grain size, and calcined for two hours at 660-700°C to enhance the workability and reactivity.

2.2 Geopolymers preparation

The geopolymer production involved an alkali reaction between calcined kaolin (Ck) and varying ratios of Wa (0, 10, 20, 30, 40, and 50). For preparing the alkaline solution, sodium silicate (Na_2SiO_3) solution was mixed with sodium hydroxide (NaOH, ten molars) in a one-to-one ratio. The optimal component ratio was determined through optimization. The best workability was achieved with a solid/liquid mass ratio of 2, a key finding of our research. The solid components of Ck and Wa were mixed for 5 minutes in a mechanical overhead mixer. An alkaline activator was added gradually through mixing for 10-15 minutes. The prepared mix was cast into three cubic steel moulds (5 × 5 × 5 cm) and cured at 80°C for 24 hours. The cured specimens were cooled to room temperature and de-moulded, then exposed to two conditions: room temperature for 14 days and water immersion for one day. The unconfined compressive strength was measured for air-dry specimens using a MATEST testing machine (Model NS205N) after 14 days at a constant displacement rate of 5 mm/min. Water absorption was examined for specimens immersed in tap water for 24 hours. The changes resulting from replacing the amount of Ck with 10, 20, 30, 40, and 50% Wa were thoroughly evaluated considering compressive strength, dry density, water absorption, and porosity values that were measured according to ASTM C 373. The best ratio of Wa was chosen based on physical properties to examine the geopolymer characteristics and lead removal efficiency, ensuring the reliability of our findings (Figure 1).

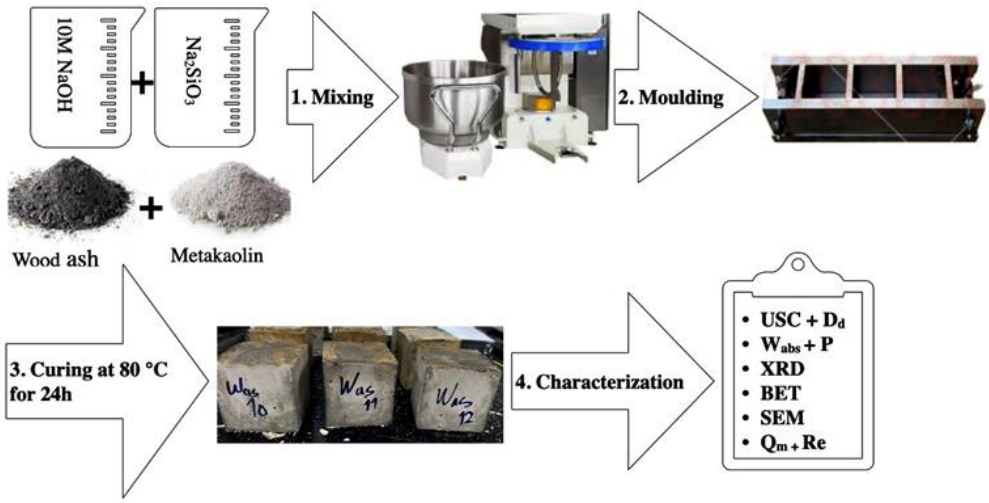

Figure 1. Geopolymers preparation steps
Note: UCS: unconfined compressive strength, D_d: dry density, W_{abs}: water absorption, P: porosity, XRD: X-ray diffraction, SSA: specific surface area, SEM: scanning electron microscope, Q_m: maximum uptake capacity, and Re: removal efficiency.

2.3 Materials and geopolymers characterization

An X-ray fluorescence type S8 Tiger from Bruker Company was used to analyze the materials' significant elements. The thermal analysis was carried out by a thermal analyzer (TG 209 F3 Tarsus) with a heating rate of 20°C/min from 50 to 1000°C under N_2 flow to obtain TG/DTA curves. An X-ray diffractometer type XRD-7000 from Shimadzu analyzed the mineral content of the used materials and selected geopolymers. Scanning electron microscope type QUANTA 600 FE-SEM was used for microstructural analysis and spot analysis by energy dispersion spectroscopy (EDS) from Bruker Company. The pore size was determined using Microtrac Belsorp Max II liquid nitrogen 77K, and the specific surface area was determined via the BET (Brunauer-Emmett-Teller) method.

2.3.1 Pb^{+2} removal from an aqueous solution

To utilize selected geopolymers with 50% Wa as an adsorbent for Pb^{+2} removal, a 100 ppm of $Pb(NO_3)_2$ solution was prepared. One gram of geopolymer powder was added to 50 ml of the prepared solution and shaken for 24 hours. The concentration of Pb^{+2} in the mix was measured using an atomic absorption spectrometer. The removal efficiency in

equilibrium was estimated using the expression below:

$$Re\% = \frac{C_0 - C_e}{C_0} \times 100\%$$

where, Re is the removal efficiency, C_0 is the initial concentration of Pb^{+2} (mg/L), and C_e is the equilibrium concentration of Pb^{+2} (mg/L).

The maximum uptake capacity of Pb^{+2} by geopolymer can be calculated based on the following equation:

$$Q_m = (C_0 - C_e) \times V/m$$

where, Q_m is the maximum uptake capacity (mg/g), V is the volume of solution (ml), and m is the geopolymer mass (g).

2.3.2 Adsorption isotherms

For Pb^{+2} removal experiments, the adsorption isotherms of Pb^{+2} on the selected geopolymer were studied using the batch equilibrium technique. 0.01g of geopolymer powder was added to 50 ml of $Pb(NO_3)_2$ solution. The mixture was shaken for 24 hours, after which it was filtered using a microfilter. The changes in Pb^{+2} concentration were investigated to study the maximum uptake capacity of Pb^{+2} from an aqueous solution. The Langmuir and Freundlich isotherms were utilized to figure out the system of adsorbent particle distribution among aqueous and adsorbent based on the following equation:

Langmuir model:

$$C_e/Q_e = 1/bQ_m + C_e/Q_m$$

Freundlich model:

$$Q_e = Kf\ C_e\ 1/n$$

where, C_e is the concentration of Pb^{+2} (mg/L) at equilibrium, Q_e (mg/g) is the amount of adsorbed Pb^{+2} at equilibrium per unit mass of adsorbent, b is a Langmuir model constant relating to the energy of adsorption, Q_m (mg/g) is the maximum uptake capacity of Pb^{+2}, C_e (mg/L) is the equilibrium concentration of Pb^{+2}. *1/n* and *Kf* are constants for the Freundlich model, indicating the intensity of adsorption and their capacity.

3. RESULTS AND DISCUSSION

3.1 Characterization of raw materials

Table 1. Major chemical composition of the used materials

Oxides%	Ck	Wa
SiO_2	61.7	4.87
TiO_2	1.73	0.75
Al_2O_3	29.9	1.68
Fe_2O_3	2.18	1.6
Mn	-	0.25
MgO	0.52	3.59
CaO	0.33	36.4
Na_2O	0.32	1.76
K_2O	0.89	16.6
P_2O_5	-	3.17
SO_3	0.28	1.93
Cl	-	0.798
L.O.I	1.85	26.14

Table 1 shows the chemical composition of Ck and Wa as obtained from the XRF analysis. The essential components for the geopolymerization process are SiO_2 and Al_2O_3. Ck mainly comprises SiO_2 (61.7%) and Al_2O_3 (29.9%). The SiO_2 content in the Ck sample corresponds to silica polymorphs, quartz and silicates, clays (kaolinite), and micas (muscovite), which are also the primary sources of Al_2O_3. CaO is the major oxide in the Wa sample, about 36.4%. As reported in previous work [27], the findings revealed that wood ash is composed of CaO (48.8 wt.%), LOI (12.2 wt.%), K_2O (10.4 wt.%), MgO (6.6 wt.%), Fe_2O_3 (5.3 wt.%), SiO_2 (4.4 wt.%), and Al_2O_3 (1.8 wt.%).

Figure 2 shows the X-ray diffraction chart of Ck. The X-ray pattern indicates that kaolinite and quartz are the most abundant minerals. Quartz primary reflections appear at 20.9°, 26.7°, and 50.2° (2θ) angles corresponding to 1.82, 3.34, and 4.25 d-spacings, respectively. Kaolinite peak appears at a 24.9° (2θ) angle corresponding to 3.58 d-spacing. The other identified mineral is muscovite. The X-ray diffractogram of Wa is illustrated in Figure 3. The results show that the major mineral constituents are calcite ($CaCO_3$), lime (CaO), and fairchildite (K_2CaCO_3). Quartz (SiO_2) and amorphous phases appear in the broad peaks. Misra et al. (1993), Etiégni and Campbell [4], Chowdhury et al. [12], and Ukrainczyk et al. [29] revealed that lime, calcite, portlandite, and calcium silicate were the main mineral phases of the wood ash. They also found that SiO_2 was present in crystalline and amorphous forms in wood ash.

The thermal stability curves of Ck and Wa are illustrated in Figure 4. Heating the Ck sample below about 600℃ has decreased the mass of the sample by 0.9%, and then, after heating to 1000℃, a relative loss in weight of 0.60% is noticed. The total weight loss was 1.5%, which agrees with the LOI obtained from the XRF results. This finding matches the results obtained by Douiri et al. [30]. Thermal gravimetric analysis of the Wa sample shows that the total weight loss at 1000ºC is about 33%. Between 550℃ and 800℃, weight loss of about 20% reveals the presence of carbon dioxide in its inorganic form. De Rossi et al. [31] found that the total loss of wood ash was about ten wt.%. 1.8 wt.% of loss related to moisture evaporation up to 250℃. Further mass loss (~1.5%) is between 250 and 500℃ due to the combustion of organic material. From 500 to 800℃, about 6% of mass loss results in $CaCO_3$ decomposition. The nitrogen adsorption-desorption isotherms of Ck and Wa are shown in Figure 5. The nitrogen sorption isotherms of Ck exhibit very low adsorption below (P/Po) = 0.2. The isotherms also exhibit some nitrogen uptake at P/Po > 0.2. Based on IUPAC (International Union of Pure and Applied Chemistry, 1986) the classification, the shape of the Ck adsorption isotherm curve characterizes type III isotherms obtained with macroporous adsorbents. Point C in the middle section of the isotherm shows the completion of the monolayer cover stage and the beginning of multilayer adsorption. It is essential to highlight that all the absorption-desorption isotherms of Wa presented a similar shape, with type IV and V isotherms indicating, as expected, a mesoporous structure. For Ck and Wa, the BET analysis showed a surface area of 15.4 m^2/g and 18.6 m^2/g, respectively. Many authors have reported that wood ash particles have a porous structure with high specific surface areas [26, 29, 32]. Rajamma et al. [26] noted that the surface area of wood ash from forest residues was about 40.29 m^2/g.

Figure 6 shows the microstructural image with spot analysis of the Ck sample. It shows the platy shape and micrometric

size of the kaolinite particles. The typical laminar appearance of these phyllosilicates is observed, in addition to silica-rich aggregates corresponding to quartz. The SEM micrograph of Wa is shown in Figure 7. As Ukrainczyk et al. [29] reported, it reveals irregular shapes and porous particles.

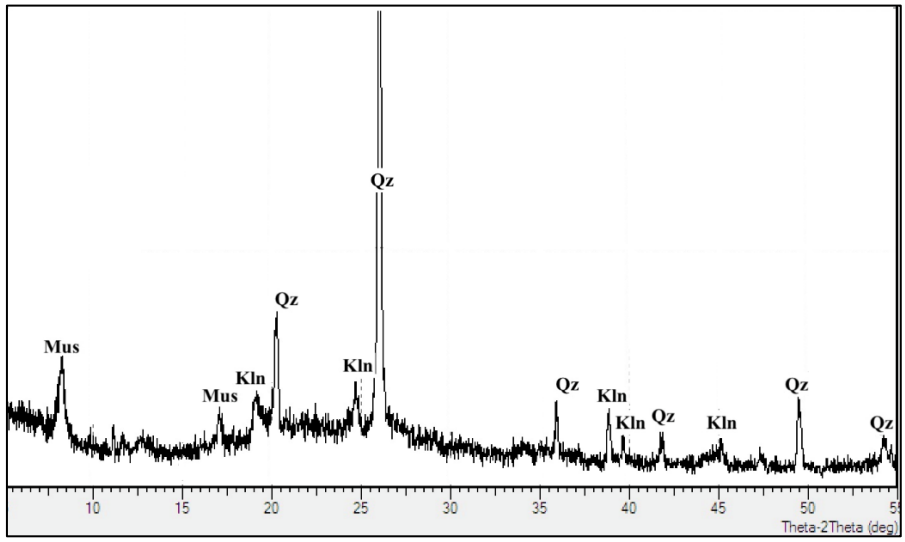

Figure 2. XRD spectrum of Ck
Note: Qz: quartz, Mus: muscovite, and Kln: kaolinite

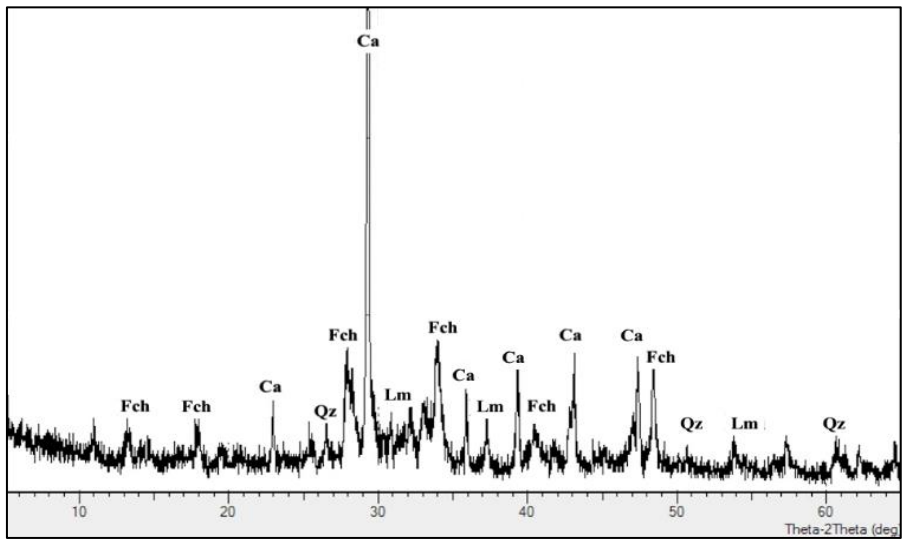

Figure 3. XRD spectrum of Wa
Note: Lm: lime, Ca: calcite, Qz: quartz, and Fch: fairchildite

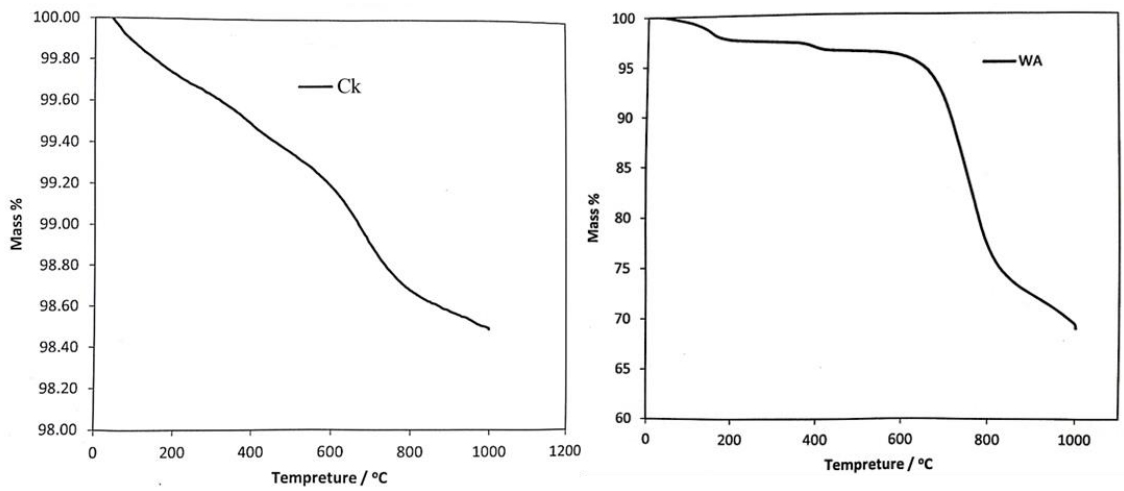

Figure 4. Thermal stability curves of Ck and Wa

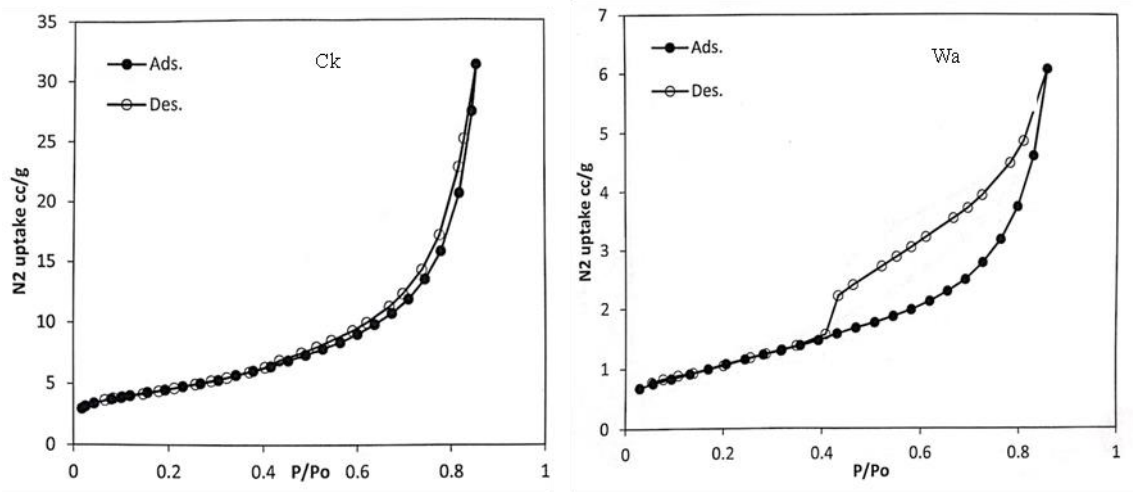

Figure 5. Adsorption/desorption curves of Ck and Wa

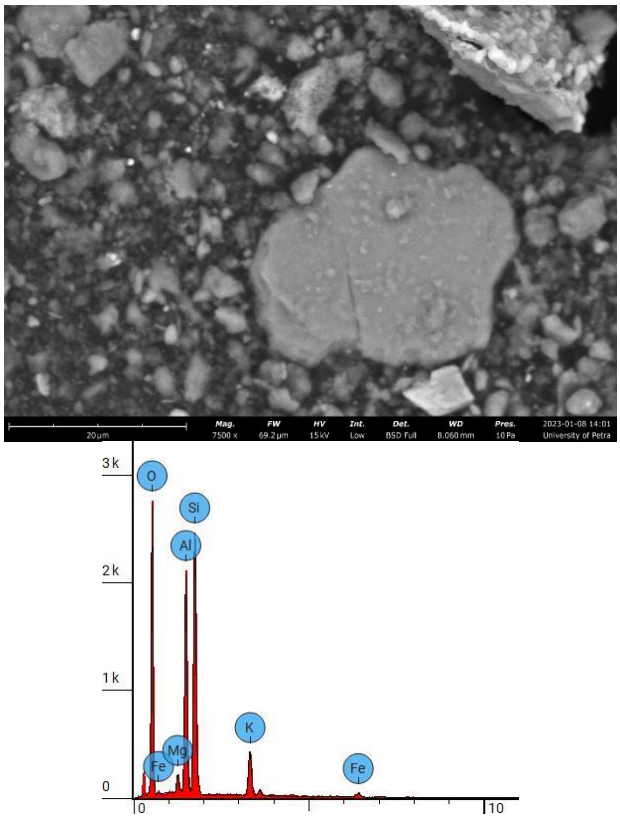

Figure 6. Microstructural image with spot analysis of Ck

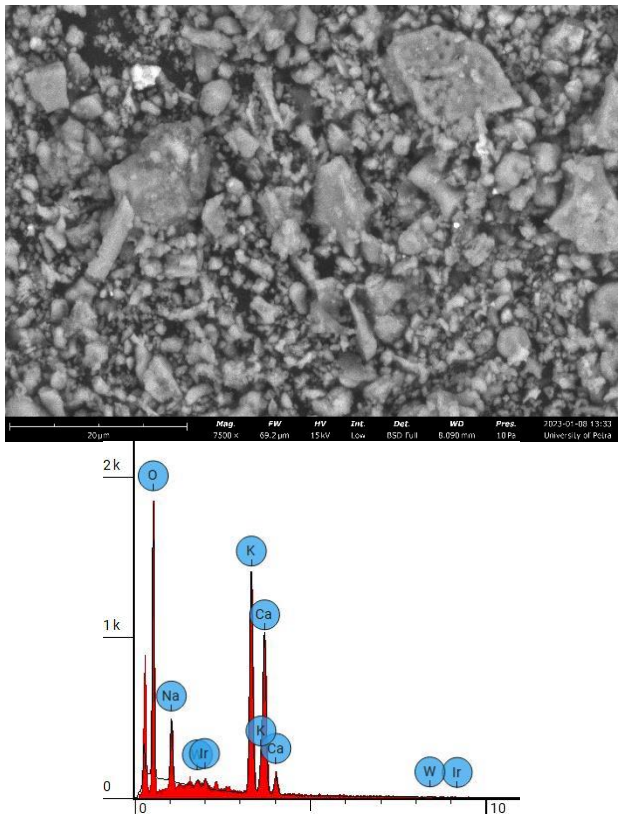

Figure 7. Microstructural image with spot analysis of Wa

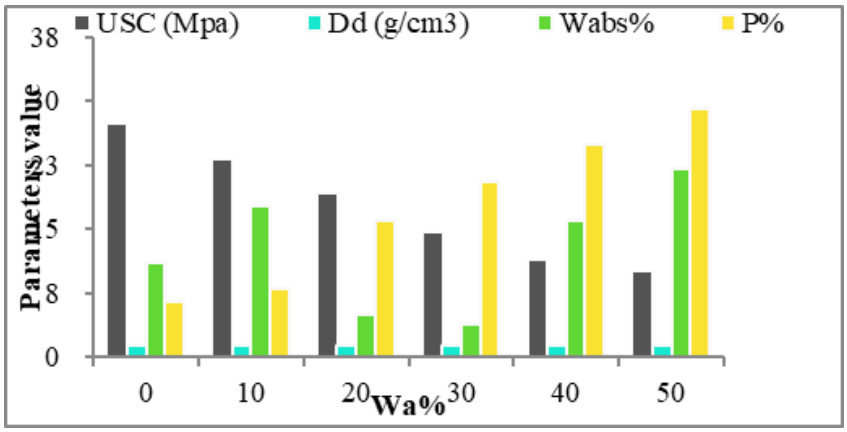

Figure 8. Variations in physical characteristics versus Wa%

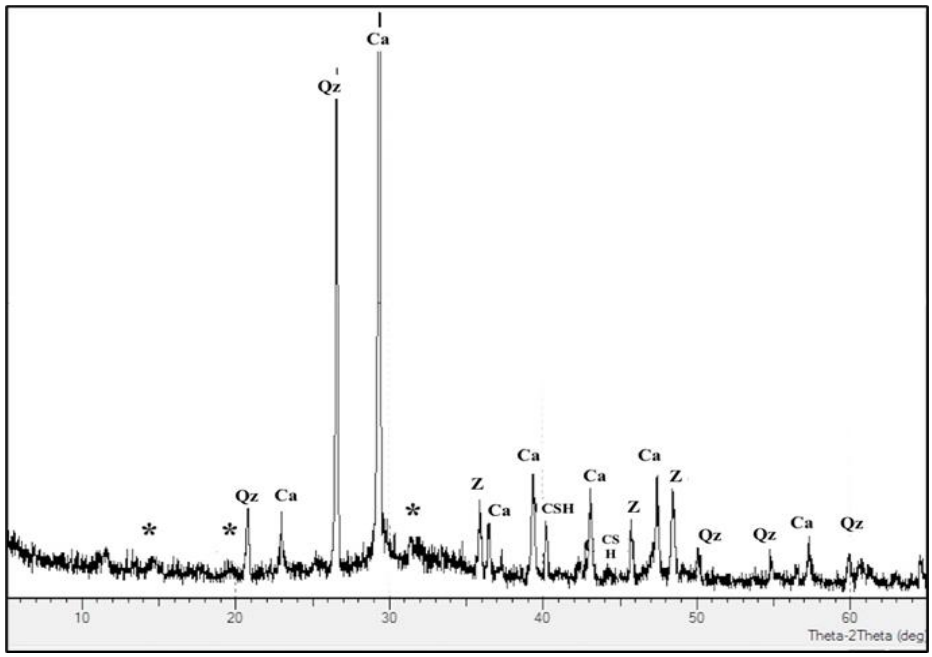

Figure 9. XRD pattern of geopolymer with 50% Wa
Note: *: amorphous phase, Qz: quartz, Z: zeolite, Ca: calcite, and CSH: calcium-silicate hydrate

3.2 Characterization of synthesized geopolymers

The effects of mixing different ratios of Wa to Ck during the alkali reaction are reflected in changing the physical characteristics of water absorption (W_{abs}), porosity (P), dry density (Dd), and unconfined compressive strength (UCS). Figure 8 shows that the percentage of water absorption and porosity increased almost linearly with increasing Wa ratios, from 11% and 6.38% to 22.15% and 29.13%, respectively, by increasing Wa from zero to 50%. On the other hand, dry density and compressive strength almost decreased linearly from 1.4 g/cm^3 and 27.36 MPa to 1.3 g/cm^3 and 9.95 MPa, respectively. Similar results were achieved by Catauro et al. [3]. They found that increasing the wood ash proportion reduced geopolymer densities from 1.96 g/cm^3 for 10% Wa to 1.49 g/cm^3 for 30% Wa. The evaluated mechanical strength decreased from 45 MPa to 17 MPa by increasing the Wa content from 10% to 30%, respectively. From the previous, the best Wa ratio added during geopolymers synthesis is 50%, which gives the highest porosity and water absorption values.

The XRD spectrum of the synthesized geopolymer with the best ratio of Wa (50%) are presented in Figure 9. The development of new crystalline phases was observed in crystalline zeolite and CSH. Quartz and calcite peaks still appeared due to an incomplete reaction. After geopolymerization, the crystalline phases of aluminosilicates were dissolved in an alkaline medium, forming new sodium-aluminosilicate phases (zeolitic phases). The kaolinite peak declined after geopolymerization. Geopolymer displays amorphous phases in the 2θ range of 32°-35°, with crystalline peaks at 36°, 40.5°, 46°, and 48.5°.

The photomicrograph of the synthesized geopolymer is presented in Figure 10. The development of new crystalline and amorphous phases was observed. The geopolymerization process affected the microstructure, which appeared in massive, irregular, and agglomerated forms. The random distribution of numerous micropores on the surface of the synthesized geopolymer was influential in increasing the surface area and adsorption capability. The raw wood ash contains significant CaO, causing pozzolanic and hydraulic reactions with water [33]. Thus, the alkali reaction forms Ca-Al-Si gel, producing microstructural porosity [34]. The increased pore surface areas indicate the increased porosity [35].

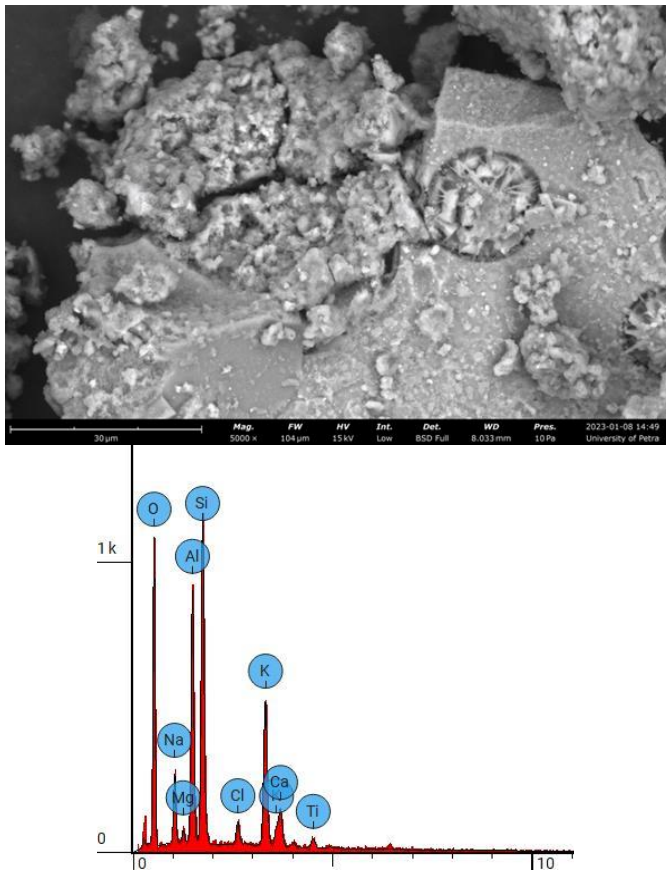

Figure 10. Microstructural image with spot analysis of geopolymer

The nitrogen adsorption-desorption isotherms of the

geopolymer sample are shown in Figure 11. The BET plot indicated the existence of a type IV isotherm as a mesoporous structure. According to the IUPAC (1986) classification, type IV occurs on porous adsorbents with 1.5-100 nm pores. At 0.5 pressure, the slope shows increased adsorbate uptake as pores become filled. The inflection point typically occurs near the completion of the first monolayer. The BET method demonstrated a surface area of 23.1 m^2/g for geopolymer, significantly more significant than the values for the raw materials. Rasaki et al. [36] reported that the surface area of fly ash geopolymer was about 16.2 m^2/g.

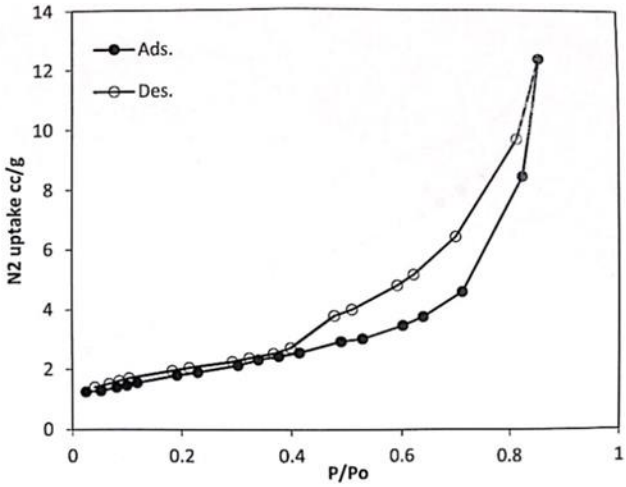

Figure 11. Adsorption/desorption curves of geopolymer

3.2.1 Pb^{+2} removal from an aqueous solution

The removal efficiency (Re) and the maximum uptake capacity (Q_m) of Pb^{+2} by raw materials and geopolymer from an aqueous solution are shown in Table 2. According to the results, the developed geopolymer with 50% wood ash has a removal efficiency of 99% and a maximum uptake capacity of 1666.67 mg/g, higher than the raw materials. According to Al-Zboon et al. [37], the developed fly ash geopolymer exceeds raw fly ash's capacity for metal uptake due to its well-defined pore size distribution and large surface area. Wang et al. [38] demonstrated that the fly ash geopolymer has a high adsorption capacity, which is due to its large surface area and porous structure.

Table 2. The maximal uptake capacity (Q_m) and removal efficiency (Re) of Pb^{+2} by raw materials and geopolymer

Materials	Q_m (mg/g)	Re%
Ck	97.09	46
Wa	1428.57	94
Geopolymer	1666.67	99

3.2.2 Adsorption isotherms

The adsorption isotherm illustrates the equilibrium interaction between Pb^{+2} and the geopolymer powder as an adsorbent. Isotherms describe the efficiency of the adsorbent. The results of coefficients of correlation (R^2), slope, and intercept values for the Langmuir and Freundlich models are shown in Table 3. Langmuir's model proposed homogeneous and monolayer adsorption processes. Freundlich's model assumed multilayer adsorption over the heterogeneous surface. The R^2 of the Langmuir model was more significant than the Freundlich model for raw materials and geopolymer. Results indicated that the Langmuir adsorption isotherm was the best model for Pb^{+2} adsorption, with R^2 of 0.998. This relates to the pore structure described in the geopolymer's SEM image. The pore structure increased the adsorbent's porosity, causing the adsorbate to adsorb onto the surface more effectively. Prabhakar et al. [28] and El Alouani et al. [39] reported similar findings. According to Al-Ghouti et al. [40], it can be assumed that the substitution caused the adsorbate surface to be opposite, allowing for electrostatic contact between the adsorbent surface and the adsorbed metal.

Table 3. The results of R^2, slop, and intercept values for the Langmuir and Freundlich models for raw material and geopolymer

	Langmuir Isotherm			Freundlich Isotherm		
Materials	**Slop**	**Intercept**	R^2	**Slop**	**Intercept**	R^2
Ck	0.0007	0.0016	0.943	0.1161	2.945	0.468
Wa	0.0103	1.0583	0.957	0.1517	1.485	0.579
Geopolymer	0.0006	0.0019	0.998	0.1197	2.844	0.733

4. CONCLUSION

The utilization of wood ash for geopolymer production has been successful by the chemical reaction of wood ash and calcined kaolin in an alkali solution. The best ratio of wood ash was 50% based on the physical characteristics. The generated geopolymer has zeolitic and amorphous phases and shows structural micropores. It was found that the selected geopolymer had a higher removal efficiency and absorbing capacity of Pb^{+2} in an aqueous solution than the raw materials. The study of isotherm adsorption of Pb^{+2} on geopolymers showed that the Langmuir model performed better than the Freundlich models in describing adsorption. It represents the homogeneity of adsorption. Further research will be in progress shortly to evaluate the effect of adding wood ash on the properties of geopolymers and for removing other pollutants.

ACKNOWLEDGMENT

The authors thank The Hashemite University's Deanship of Scientific Research for their financial support and the Royal Scientific Society's lab technicians for contributing to this effort through laboratory work and analysis.

REFERENCES

[1] Campbell, A.G. (1990). Recycling and disposing of wood ash. Tappi Journal, 73(9): 141-146.

[2] Properzi, M., Pattis, R., Pichelin, F. (2008). Wood ash as a resource for the production of innovative composite materials. https://arbor.bfh.ch/id/eprint/11617.

[3] Catauro, M., Viola, V., D'Amore, A. (2023). Mosses on geopolymers: Preliminary durability study and chemical

characterization of metakaolin-based geopolymers filled with wood ash. Polymers, 15(7): 1639. https://doi.org/10.3390/polym15071639

[4] Etiegni, L., Campbell, A.G. (1991). Physical and chemical characteristics of wood ash. Bioresource Technology, 37(2): 173-178. https://doi.org/10.1016/0960-8524(91)90207-Z

[5] Jacobson, S., Lundström, H., Nordlund, S., Sikström, U., Pettersson, F. (2014). Is tree growth in boreal coniferous stands on mineral soils affected by the addition of wood ash? Scandinavian Journal of Forest Research, 29(7): 675-685. https://doi.org/10.1080/02827581.2014.959995

[6] Huotari, N., Tillman-Sutela, E., Moilanen, M., Laiho, R. (2015). Recycling of ash-For the good of the environment? Forest Ecology and Management, 348: 226-240. https://doi.org/10.1016/j.foreco.2015.03.008

[7] Hannam, K.D., Venier, L., Allen, D., Deschamps, C., Hope, E., Jull, M., Kwiaton, M., McKenney, D., Rutherford, P.M., Hazlett, P.W. (2018). Wood ash as a soil amendment in Canadian forests: What are the barriers to utilization? Canadian Journal of Forest Research, 48(4): 442-450. https://doi.org/10.1139/cjfr-2017-0351

[8] Romdhane, L., Ebinezer, L.B., Panozzo, A., Barion, G., Dal Cortivo, C., Radhouane, L., Vamerali, T. (2021). Effects of soil amendment with wood ash on transpiration, growth, and metal uptake in two contrasting maize (Zea mays L.) hybrids to drought tolerance. Frontiers in Plant Science, 12: 661909. https://doi.org/10.3389/fpls.2021.661909

[9] Tarun, R.N., Rudolph, N.K., Rafat, S. (2003). Use of wood ash in cement-based materials. A CBU Report, CBU-2003-19 (REP-513).

[10] Ban, C.C., Ramli, M. (2012). Characterisation of high calcium wood ash for use as a constituent in wood ash-silica fume ternary blended cement. Advanced Materials Research, 346: 3-11. https://doi.org/10.1016/j.enbuild.2015.07.016

[11] Siddique, R. (2012). Utilization of wood ash in concrete manufacturing. Resources, Conservation and Recycling, 67: 27-33. https://doi.org/10.1016/j.resconrec.2012.07.004

[12] Chowdhury, S., Mishra, M., Suganya, O.M. (2015). The incorporation of wood waste ash as a partial cement replacement material for making structural grade concrete: An overview. Ain Shams Engineering Journal, 6(2): 429-437. https://doi.org/10.1016/j.asej.2014.11.005

[13] Elahi, M., Qazi, A.U., Yousaf, M., Akmal, U. (2015). Application of wood ash in the production of concrete. Science International, 27: 1277-1280.

[14] Siqueira, F.B., Holanda, J.N.F. (2013). Reuse of grits waste for the production of soil-cement bricks. Journal of Environmental Management, 131: 1-6. https://doi.org/10.1016/j.jenvman.2013.09.040

[15] Ribeiro, S.V. (2017). Reuse of wood ash waste in the production of soil-cement brick: Formulation, properties and microstructure. Doctoral Thesis, UENF, Campos Goytacazes. https://doi.org/10.1590/0366-69132022683853052

[16] Chen, C., Wu, H. (2018). Lightweight bricks manufactured from ground soil, textile sludge, and coal ash. Environmental Technology, 39(11): 1359-1367. https://doi.org/10.1080/09593330.2017.1329353

[17] Souza, P.C., Nascimento, E.S.S., Melo, L., Oliveira, H.A., Almeida, V.G.O., Melo, F.M.C. (2022). Study for the incorporation of wood ash in soil-cement brick. Cerâmica, 68: 38-45. https://doi.org/10.1590/0366-69132022683853052

[18] Temuujin, J., Surenjav, E., Ruescher, C.H., Vahlbruch, J. (2019). Processing and uses of fly ash addressing radioactivity (Critical review). Chemosphere, 216: 866-882. https://doi.org/10.1016/j.chemosphere.2018.10.112

[19] Cheah, C.B., Part, W.K., Ramli, M. (2015). The hybridizations of coal fly ash and wood ash for the fabrication of low alkalinity geopolymer load bearing block cured at ambient temperature. Construction and Building Materials, 88: 41-55. https://doi.org/10.1016/j.conbuildmat.2015.04.020

[20] Cheah, C.B., Samsudin, M.H., Ramli, M., Part, W.K., Tan, L.E. (2017). The use of high calcium wood ash in the preparation of Ground granulated blast furnace slag and pulverized fly ash geopolymers: A complete microstructural and mechanical characterization. Journal of Cleaner Production, 156: 114-123. https://doi.org/10.1016/j.jclepro.2017.04.026

[21] Candamano, S., De Luca, P., Frontera, P., Crea, F. (2017). Production of geopolymeric mortars containing forest biomass ash as partial replacement of metakaolin. Environments, 4(4): 74. https://doi.org/10.3390/environments4040074

[22] Abdulkareem, O.A., Ramli, M., Matthews, J.C. (2019). Production of geopolymer mortar system containing high calcium biomass wood ash as a partial substitution to fly ash: An early age evaluation. Composites Part B: Engineering, 174: 106941. https://doi.org/10.1016/j.compositesb.2019.106941

[23] Owaid, H.M., Al-Rubaye, M.M., Al-Baghdadi, H.M. (2021). Use of waste paper ash or wood ash as substitution to fly ash in production of geopolymer concrete. Przegląd Naukowy Inżynieria i Kształtowanie Środowiska, 30(3): 464-476. https://doi.org/10.22630/PNIKS.2021.30.3.39

[24] Silvestro, L., Scolaro, T.P., Ruviaro, A.S., dos Santos Lima, G.T., Gleize, P.J.P., Pelisser, F. (2023). Use of biomass wood ash to produce sustainable geopolymeric pastes. Construction and Building Materials, 370: 130641. https://doi.org/10.1016/j.conbuildmat.2023.130641

[25] Teker Ercan, E.E., Cwirzen, A., Habermehl-Cwirzen, K. (2023). The effects of partial replacement of ground granulated blast furnace slag by ground wood ash on alkali-activated binder systems. Materials, 16(15): 5347. https://doi.org/10.3390/ma16155347

[26] Rajamma, R., Labrincha, J.A., Ferreira, V.M. (2012). Alkali activation of biomass fly ash-metakaolin blends. Fuel, 98: 265-271. https://doi.org/10.1016/j.fuel.2012.04.006

[27] Bijeljić, J., Ristić, N., Grdić, D., Pavlović, M. (2023). Possibilities of biomass wood ash usage in geopolymer mixtures. Tehnički Vjesnik, 30(1): 52-60. https://doi.org/10.17559/TV-20220215222503

[28] Prabhakar, A.K., Mohan, B.C., Tai, M.H., Yao, Z., Su, W., Teo, S.L.M., Wang, C.H. (2023). Green, non-toxic and efficient adsorbent from hazardous ash waste for the recovery of valuable metals and heavy metal removal from waste streams. Chemosphere, 329: 138524.

https://doi.org/10.1016/j.chemosphere.2023.138524
[29] Ukrainczyk, N., Vrbos, N., Koenders, E.A. (2016). Reuse of woody biomass ash waste in cementitious materials. Chemical and Biochemical Engineering Quarterly, 30(2): 137-148. https://doi.org/10.15255/CABEQ.2015.2231
[30] Douiri, H., Louati, S., Baklouti, S., Arous, M., Fakhfakh, Z. (2016). Enhanced dielectric performance of metakaolin-H3PO4 geopolymers. Materials Letters, 164: 299-302. https://doi.org/10.1016/j.matlet.2015.10.172
[31] De Rossi, A., Simão, L., Ribeiro, M.J., Hotza, D., Moreira, R.F.P.M. (2020). Study of cure conditions effect on the properties of wood biomass fly ash geopolymers. Journal of Materials Research and Technology, 9(4): 7518-7528. https://doi.org/10.1016/j.jmrt.2020.05.047
[32] Carević, I., Štirmer, N., Trkmić, M., Kostanić Jurić, K. (2020). Leaching characteristics of wood biomass fly ash cement composites. Applied Sciences, 10(23): 8704. https://doi.org/10.3390/app10238704
[33] Ahmaruzzaman, M. (2010). A review on the utilization of fly ash. Progress in Energy and Combustion Science, 36(3): 327-363. https://doi.org/10.1016/j.pecs.2009.11.003
[34] Xu, H., Van Deventer, J.S.J. (2000). The geopolymerisation of alumino-silicate minerals. International Journal of Mineral Processing, 59(3): 247-266. https://doi.org/10.1016/S0301-7516(99)00074-5
[35] Luukkonen, T., Tolonen, E.T., Runtti, H., Kemppainen, K., Lassi, U. (2016). Development of efficient sorbents by alkali-treatment of high-calcium-content fly ash from the paper industry. In 4th International Conference on Sustainable Solid Waste Management, Limassol, Cyprys.
[36] Rasaki, S.A., Bingxue, Z., Guarecuco, R., Thomas, T., Minghui, Y. (2019). Geopolymer for use in heavy metals adsorption, and advanced oxidative processes: A critical review. Journal of Cleaner Production, 213: 42-58. https://doi.org/10.1016/j.jclepro.2018.12.145
[37] Al-Zboon, K., Al-Harahsheh, M.S., Hani, F.B. (2011). Fly ash-based geopolymer for Pb removal from aqueous solution. Journal of Hazardous Materials, 188(1-3): 414-421.
[38] Wang, R., Wang, J., Dong, T., Ouyang, G. (2020). Structural and mechanical properties of geopolymers made of aluminosilicate powder with different SiO_2/Al_2O_3 ratio: Molecular dynamics simulation and microstructural experimental study. Construction and Building Materials, 240: 117935. https://doi.org/10.1016/j.conbuildmat.2019.117935
[39] El Alouani, M., Alehyen, S., El Achouri, M., Taibi, M.H. (2019). Comparative study of the adsorption of micropollutant contained in aqueous phase using coal fly ash and activated coal fly ash: Kinetic and isotherm studies. Chemical Data Collections, 23: 100265. https://doi.org/10.1016/j.cdc.2019.100265
[40] Al-Ghouti, M.A., Khan, M., Nasser, M.S., Al Saad, K., Ee Heng, O.O.N. (2020). Application of geopolymers synthesized from incinerated municipal solid waste ashes for the removal of cationic dye from water. Plos One, 15(11): e0239095. https://doi.org/10.1371/journal.pone.0239095